Strong Coupling between Diffusive and Elastic Instabilities in Directional Solidification

Isabelle Durand,[1] Klaus Kassner,[2,*] Chaouqi Misbah,[1] and Heiner Müller-Krumbhaar[3]
[1]*Laboratoire de Spectrométrie Physique, Université Joseph Fourier (Centre National de la Recherche Scientifique), Grenoble I, B.P. 87, Saint-Martin d'Hères, 38402 Cedex, France*
[2]*Institut Laue-Langevin, BP 156, F-38042 Grenoble, Cedex 09, France*
[3]*Institut für Festkörperforschung des Forschungszentrums Jülich, 52425 Jülich, Germany*
(Received 26 December 1995)

We discover that a weak uniaxial stress of the order of 10^{-3} bar leads to a dramatic change of the Mullins-Sekerka instability. The threshold together with the microstructure scale are shifted by amounts going up to one (or several) decade(s). This effect should open new lines of both experimental and theoretical inquiries.

PACS numbers: 81.10.Aj, 68.70.+w, 05.70.Fh, 81.30.Fb

A moving solidification front in an external thermal gradient (directional solidification) is well known to undergo a morphological Mullins-Sekerka (MS) instability [1] above a critical growth velocity. The initially planar interface bifurcates into a cellular structure which itself bifurcates into deep cells and then to dendrites at higher speed [2]. The cellular structure may also at both small [3] and large speeds [4] experience symmetry-breaking instabilities leading ultimately to spatiotemporal chaos. The scale of the patterns is roughly determined by $\lambda_{\mathrm{MS}} \sim \sqrt{l d_0}$, which is a compromise between two competing scales: the destabilizing diffusion length $l \sim D/V$ (where V is the pulling speed and D the solute diffusion constant) and the chemical capillary length $d_0 = \gamma T_M / L \Delta T$ (L is the latent heat per unit volume, γ the surface tension, T_M the melting temperature, and ΔT the temperature miscibility gap). λ lies roughly in the 10–100 μm range. More recently, Grinfeld [5] brought out the idea, which was earlier presented by Asaro and Tiller [6], that when a solid is subject to a uniaxial stress (i.e., when $\sigma_0 = \sigma_{xx} - \sigma_{zz} \neq 0$, σ_{ij} is the stress tensor), the solid-liquid (or solid vacuum) interface breaks up into a cellular structure (ATG instability). When the solid is in contact with vacuum (a situation encountered in heteroepitaxy, for example, where the lattice misfit is the source of axial stresses), the scale of the pattern is approximately given by $\lambda_{\mathrm{ATG}} \sim \gamma E / \sigma_0^2$ (E is the Young modulus). This leads to a scale in the range of 10–100 nm for typical heteroepitaxy. When the solid is in contact with its melt, however, because of the gravitational potential energy (which does not favor a corrugation), the typical length scale is expected to be of the order of the gravitational capillary length (as is the case for gravity waves) $\lambda_{\mathrm{ATG}} \sim \sqrt{\gamma / g \Delta \rho}$ (g is gravity and $\Delta \rho$ the solid-liquid densities difference). This leads to a scale in the range 0.1–1 cm. An impressive experiment was performed by Balibar *et al.* [7] on solid ^{4}He in contact with the superfluid, and has unambiguously demonstrated the ATG instability taking place on the scale of 0.7 cm. Nonlinear calculations have shown that such an instability may lead to fracture, through the external stress is as small as a fraction of the atmospheric pressure [8].

These front instabilities are important focuses of research on both the technological and the fundamental levels, and they seem to embrace disparate situations ranging from low dimensional nanostructures [9] (e.g., quantum dots) to geology [10]. However, from the above scale estimates one would naively expect that there is (virtually) no coupling between the MS and ATG instabilities given the disparate lengths on which they operate. We show here that in contrast there is clearly strong interaction in the case for directional solidification. Indeed the external thermal gradient G combined to other parameters plays the role of an effective gravity $g_{\mathrm{eff}} = LG/\rho_s T_M$, where ρ_s is the solid density. For typical materials we find that $g_{\mathrm{eff}} = (10^3 - 10^4) g$ (i.e., the effective gravity is several orders of magnitude larger than the real gravity). This brings down the scale of the ATG instability to the range 10–100 μm, which is in the same range as the MS scale and strong coupling between the two instabilities must be expected. An important result which emanates from our analysis is that the MS stability tongue exhibits dramatic changes in the presence of even very weak uniaxial stress, of the order of 1/1000 the atmospheric pressure. In particular, the velocity threshold is reduced by a factor of about 10, while the microstructure scale is decreased at low speed and increased at large speed by the same amount. Such an effect is clearly not devoid of experimental testability. Furthermore, a weakly nonlinear analysis shows that, contrary to the pure MS instability, at low velocity the bifurcation is *subcritical* for all partition coefficients.

For ease of presentation we consider the one-sided model, which is appropriate for most ordinary solids. In the liquid phase the reduced concentration field $u = (c - c_\infty)/\Delta c$ (Δc is the miscibility gap and c_∞ is the concentration far ahead of the front) obeys the diffusion equation written in the laboratory frame

$$\Delta u + 2 \frac{\partial u}{\partial z} = \frac{\partial u}{\partial t}, \tag{1}$$

where lengths and time are reduced by $l = 2D/V$ and $\tau = l^2/D$, respectively, D being the mass diffusion constant and V the speed at which the sample is pulled through the thermal gradient field. At the interface u is subject to the mass conservation condition

$$v_n[u - k(u - 1)] = -\frac{\partial u}{\partial n}, \tag{2}$$

where v_n is the normal growth velocity, k the partition coefficient, and $\partial/\partial n$ stands for the normal derivative. For a moving boundary there is a need for an additional condition. This follows for mass transport across the interface. For a molecularly rough interface the chemical potential difference across the front is practically small so that transport across the front simply reduces to $\Delta\mu \equiv \mu_s - \mu_l \approx 0$. $\Delta\mu$ is a function of temperature, concentration, and the stress (or strain) tensor deformation. Any virtual front displacement is associated with a chemical potential difference given in [8] (to leading order)

$$0 \approx \Delta\mu = \frac{1 - \sigma^2}{2E}(\sigma_{tt} - \sigma_{nn})^2 + \gamma\tilde{\kappa} + (T_I - T_M)\frac{L}{T_M} + c_l|m_l|\frac{L}{T_M}. \tag{3}$$

The first term accounts for the increase of the solid chemical potential due to elastic deformations (σ_{ij} is the stress tensor, where the subscripts n and t refer to the normal and tangent to the interface), the second expresses capillary effects (γ is the surface tension and κ the front curvature counted positive for a convex solid), the third one the front undercooling (T_I is the actual front temperature, T_M the melting temperature, and L the latent heat per unit volume), and the last one the concentration effect (m_l is the liquidus slope). Because we consider the thermal properties of both phases to be identical, and neglect the latent heat generation at the front, T is simply given by $T = T_M + G\zeta$ where G is the thermal gradient. Therefore Eq. (3) takes the form (in reduced units)

$$u = 1 - \frac{\zeta}{l_T} - d_0\kappa + \eta\frac{(\sigma_{tt} - \sigma_{nn})^2 - \sigma_0^2}{\sigma_0^2}, \tag{4}$$

where d_0 and l_T are the usual capillary and thermal lengths, while

$$\eta = \sigma_0^2\frac{(1 - \sigma^2)}{2E}\frac{T_M}{|m_l|\Delta c L}. \tag{5}$$

In Eq. (4) we have subtracted from the full elastic effect the contribution corresponding to the prestrained situation. σ_0 is the applied uniaxial stress $\sigma_0 \equiv \sigma_{xx} - \sigma_{zz}$, and σ is the Poisson ratio. The parameter η is associated with elasticity. It measures the ratio of the elastic energy stored due to the uniaxial stress over the latent heat of melting which is involved to "jump" the temperature gap ΔT.

Now we must solve the elastic problem in the solid which is bounded by a deformable solid-liquid interface. For one dimensional deformations considered here it is convenient to make use of the Airy function χ which is related to the stress tensor by $\sigma_{xx} = \partial^2\chi/\partial z^2$, $\sigma_{zz} = -\partial^2\chi/\partial x\partial z$, and $\sigma_{zz} = \partial^2\chi/\partial x^2$. It can be shown [11] from the Lamé equation that χ obeys the biharmonic equation

$$\nabla^2\nabla^2\chi = 0. \tag{6}$$

Because we take the prestrained situation as a reference, χ must obey the condition $\chi(z \to -\infty) = 0$. Once χ is obtained, we immediately get σ_{ij}. The elastic problem must be supplemented with mechanical equilibrium conditions at the front. These are $\sigma_{nn} = -p_l$ and $\sigma_{nt} = 0$ where p_l is the hydrostatic liquid pressure, and $\sigma_{nn} = n_i\sigma_{ij}n_j$, $\sigma_{nt} = n_i\sigma_{ij}t_j$ (repeated indices are to be summed over).

Before proceeding further some remarks are in order. (i) We have neglected capillary effects in the above mechanical equilibrium condition ($\sigma_{nn} = -p_l$). It can be shown that this is legitimate up to corrections of the order of σ_0/E which is large only close to the fracture threshold. (ii) We consider the static version of elasticity, which is obviously legitimate for small velocities as compared to the sound speed. (iii) An important point which must be emphasized concerns the elastic effect due to the incorporation of the solute in the solid. This should basically alter the equilibrium condition which relates the concentration on both phases. As shown by Davis *et al.* [12], this leads to small effects on the stability diagram for typical situations.

The above set of equations supports a planar front solution moving at a constant speed. Because of elastic effects the front position undergoes a recession (compared to the unstrained situation; the stress makes the solid unfavorable, thus a melting process occurs) given by $\delta\zeta = \eta l_T$ (all lengths being measured in the diffusion length unit). For moderate uniaxial stresses ($\sigma_0 \sim 0.01$ bar) this recession is of the order of $0.1 l_T$. Usually $l_T \sim 100\ \mu$m so that the recession is of the order of 10 μm. The linear stability analysis is easily accomplished. The diffusion problem is standard and shall not be reproduced here. For the elastic problem the biharmonic equation leads to a solution of the form $\chi = \epsilon(a + bz)e^{qz+\omega t+iqx}$, where ϵ is the deformation amplitude, q is the perturbation wavelength, and ω is the amplification (attenuation) rate that we wish to determine. Mechanical equilibrium imposes $a = 0$ and $b = -\sigma_0$. Reporting this solution into (4), and again together with the diffusion field into Eqs. (1) and (2), we obtain two homogeneous sets of two equations for the deformation and the diffusion field amplitudes. The compatibility condition leads to the dispersion relation

$$\omega + 2 = (1 - 2k)X + (2 - X)\sqrt{1 + q^2 + \omega}, \tag{7}$$

where $X = l_T^{-1} - 4\eta q + d_0 q^2$. For $\eta = 0$ we recover the Mullins-Sekerka dispersion relation. For a vanishing growth velocity we immediately get from the above dispersion relation $\omega = \sqrt{q^2 + \omega}\,(4\eta q - 1/l_T - d_0 q^2)$ which is the dynamical version of the ATG result when bulk dissipation prevails. Note that Eq. (7) could be inferred directly by combining the MS and ATG results.

It can be shown analytically [13] that $\mathrm{Re}(\omega) = 0$ entails automatically that $\mathrm{Im}(\omega) = 0$. That is to say, the bifurcation is steady. Figure 1 shows the neutral curve (solid line) and the most dangerous mode (dashed line) for $\eta = 0$ (thin lines) and $\eta = 0.0014$ (thick lines) (other parameters are shown in the caption). For typical parameter values we find that $\eta = 10^{-3}$ corresponds to a uniaxial stress $\sigma \sim 10^{-3}$ bar, which is a small fraction of the atmospheric pressure.

A striking result is that, despite the small value of the external stress, the neutral curve exhibits unexpected changes. For example, both the upper and lower limits of the threshold are, respectively, about 10 times smaller and larger than the MS ones (note that the scales are logarithmic). The same holds for the scale of the most dangerous modes close to the upper and lower limits. Here elasticity favors small scales at low speed and large scales at high speed. From Eq. (7) we find after some algebraic manipulations that the lower velocity threshold value in the tongue is given (in physical variables shown here with tildes)

$$V_{c1} = \frac{D}{\tilde{l}_T}\left(1 - 4\,\frac{\eta^2 \tilde{l}_T}{\tilde{d}_0}\right). \tag{8}$$

Since η can reach values (at the threshold) going up to 10^{-2}, it is easily visible (because typically $\tilde{l}_T/\tilde{d}_0 \sim 10^5$) that the ratio $4\tilde{l}_T\eta^2/\tilde{d}_0$ can be very close to unity for uniaxial stresses of the order of 10^{-3} bar. In the extreme limit where $\eta^2 > \tilde{d}_0/4\tilde{l}_T$, there is no threshold: The interface is absolutely unstable at all velocities. The reduced bifurcation wave number at the lower threshold is large compared to unity and obeys the equation $q_{c1} = [2k/(d_0 - 2\eta/q_{c1})]^{1/3}$. Inspection of this equation leads to a physical wave number which behaves as $\tilde{q}_{c1} \simeq 2\eta/\tilde{d}_0 + (k\tilde{d}_0/8D^2\eta^2)V^2$. The first part is purely elastic and is independent of V, while the second one is a mixture of elasticity and diffusion. Note that in the pure MS case $q_c \sim V^{3/4}$. Elasticity leads to a completely different scaling with V. We can see also in Fig. 1 that for V small the line of the most dangerous mode is concave in the presence of a uniaxial stress, and it is convex otherwise.

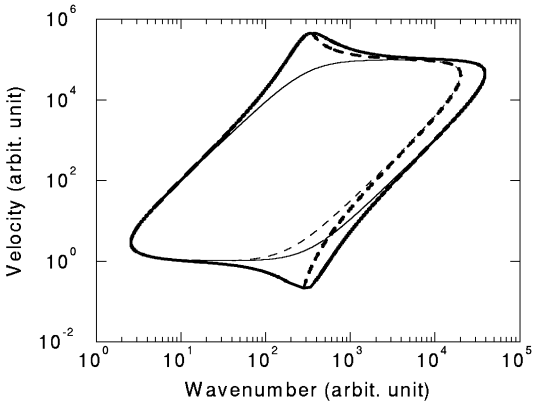

FIG. 1. The neutral curve (solid line) and the most dangerous mode (dashed line) in the presence of a uniaxial stress (thick line) in the plane (physical wave number, physical velocity) compared to the unstrained case (thin line). Here $\eta = 0.0014$, $d_0 = 10^{-5}$, $k = 1$, and units are chosen so that $l_T = 1$ and $D = 1$.

In the large velocity regime $q \ll 1$, we obtain that the upper threshold is given by

$$V_{c2} = \frac{D}{k(\tilde{d}_0 - 4\eta^2\tilde{l}_T)}. \tag{9}$$

Here again there is no restabilization if $\eta^2 > \tilde{d}_0/4\tilde{l}_T$. The (reduced) bifurcation wave number is given in this limit by $\tilde{q}_{c2} = 2\eta/(\tilde{d}_0 - l/2k)$. Upon substitution of the relation (9), we obtain $\tilde{q}_{c2} = 1/(2\eta\tilde{l}_T)$ (recall that at the upper limit $q \to 0$ in the absence of stress and for a vanishing thermal gradient).

If the tongue is preserved (i.e., $\eta^2 < 4\tilde{d}_0/\tilde{l}_T$) and for typical values given in the caption of Fig. 1, we find that $V_{c1}/V_{\mathrm{MS1}} \sim 7$, $q_{c1}/q_{c\mathrm{MS1}} \sim 4$, while $V_{c2}/V_{\mathrm{MS2}} \sim 40$, $q_{c2}/q_{c\mathrm{MS2}} \sim 20$, where the subscript "MS" refers to the bare Mullins-Sekerka value. The fact that the elastic effect is much more pronounced in the large velocity regime is understood as follows. At large velocity the diffusion length becomes smaller and smaller. The self-interaction of the front becomes local and usually capillary effects overcome the diffusive instability. Since elasticity acts always on large scales, it wins over diffusion and determines the dynamics at large scales (q small).

We have analyzed the weakly nonlinear behavior in order to determine the nature of the bifurcation. We give here simply the result, while details will be published elsewhere. The pure ATG instability is known to be subcritical [14]. The Mullins-Sekerka instability may be subcritical or supercritical depending on the velocity and the partition coefficient. For small velocities the MS bifurcation is subcritical [15] for $k < 0.4$ (which is the case for the majority of metals) and supercritical otherwise. Here we find that in the small V or equivalently large q regime the (3rd order) Landau constant is dominated by the ATG effect which behaves as q^4; the MS effect behaves as q^2. That is to say, the bifurcation is subcritical for all partition coefficients.

Finally, an important task concerns the experimental testability of our finding. A possibility would be to use a cell with piezoelectric plates in order to impose a controlled uniaxial stress on the solid as has been devised for ^{4}He by Balibar *et al.* [7]. Transparent materials such as succinonitrile are not, in our opinion, suitable since

these have plastic properties. This does not mean so far that plastic behaviors may not lead to interesting features. But this question is beyond the present study. Of course, transparent materials have interesting properties such as the allowance for an *in situ* analysis, and it would be very important to take advantage of that. However, many materials that enter this category are, beside plasticity, smooth on the atomic scale, and that therefore exhibit faceted morphologies. In contrast, many metallic alloys are rough on the atomic scale and lead to rounded growth shapes. We believe that metallic alloys are important candidates on which to perform such experiments. There exists by now overabundant literature about directional solidification on these materials. The effects we put forward should be easily detectable since they involve strong changes on both the threshold values and the scales of the pattern.

We believe that experimental checks of our theory are decisive in order to guide further developments.

C. M. is grateful to C. Caroli for fruitful discussions. This work was completed while C. M. was visiting the Forschungszentrum at Jülich. He acknowledges the hospitality of the center and the financial support from the Alexander-von-Humboldt association. K. K. and C. M. benefited from financial support under NATO Grant No. CRG.920541.

*Permanent address: Institut fuer Theoretische Physik, Otto-von-Guericke-Universität Magdeburg, Postfach 4120, D-39016 Magdeburg, Germany.

[1] W. W. Mullins and R. F. Sekerka, J. Appl. Phys. **35**, 444 (1964).
[2] H. Esaka and W. Kurz, J. Cryst. Growth **72**, 578 (1985).
[3] S. de Cheveigné, and C. Guthmann, J. Phys. I (France) **2**, 193 (1992); J. T. C. Lee, and R. A. Brown, Phys. Rev. B **47**, 4937 (1993).
[4] K. Kassner, C. Misbah, H. Müller-Krumbhaar, and A. Valence, Phys. Rev. E **49**, 5477 (1994); **49**, 5495 (1994).
[5] M. A. Grinfeld, Dokl. Akad. Nauk. SSSR **290**, 1358 (1986) [Sov. Phys. Dokl. **31**, 831 (1986)].
[6] R. J. Asaro and W. A. Tiller, Metall. Trans. **3**, 1789 (1972).
[7] S. Balibar, D. O. Edwards, and W. F. Saam, J. Low Temp. Phys. **82**, 119 (1991); R. H. Torri and S. Balibar, J. Low Temp. Phys. **89**, 391 (1992).
[8] K. Kassner and C. Misbah, Europhys. Lett. **28**, 245 (1994).
[9] R. Nötzel, J. Temmyo, and T. Tamamura, Nature (London) **369**, 131 (1994).
[10] S. R. Tait and C. Jaupart, in *Interactive Dynamics of Convection and Solidification*, edited by H. Davis, H. E. Huppert, U. Müller, and M. G. Worster, ASI, Ser. E (Kluwer Academic Publishers, Dordrecht, 1992).
[11] See L. D. Landau and E. Lifshitz, *Theory of Elasticity* (Mir, Moscow, 1967).
[12] B. J. Spencer, P. W. Woorhees, S. H. Davis, and G. B. McFadden, Acta Metall. Mater. **40**, 1599 (1992).
[13] I. Durand, K. Kassner, and C. Misbah (unpublished).
[14] P. Nozières, J. Phys. I (France) **3**, 681 (1993). Some interesting aspects of the heat current and its role acting as an effective gravity was pointed out to us by P. Nozières after this work was submitted; see R. M. Bowley and P. Nozières, J. Phys. I (France) **2**, 433 (1992).
[15] B. Caroli, C. Caroli, and B. Roulet, J. Phys. (Paris) **43**, 1767 (1982).